International Journal of Science and Research (IJSR)
ISSN (Online): 2319-7064
Index Copernicus Value (2015): 78.96 | Impact Factor (2015): 6.391

Effect of Doping Concentration of Potassium (K) on the Crystallographic and Optical Properties of Cesium Iodide Films (CsI)

Dr. Gaafar M. Moosa

Department of Basic Science, Dental College, Baghdad University

Abstract: ***In this work, we study the properties of cesium iodide (CsI) thin film as a function of potassiumdoping concentrations The X-Ray diffraction of cesium iodide shows polycrystalline in nature with centered cubic (bcc) structure. The optical transmittance of cesium iodide films has been analyzed in the spectral range from 200 nm to 800 nm. The optical gapenergy is calculated from the extrapolation of $(\alpha h\upsilon)^2$ via $(h\upsilon)$for direct transitions, the experimental data show the energy gap decrease with increasing doping concentration from3.85 to 3.79eV.***

Keywords: Cesium iodide, X-ray diffraction, grain size**.** Transmittance, Band gap energy

1. Introduction

The important parameters that determine using scintillation material are (1) Overall efficiency of x-ray-to-light conversion, (2) X-ray stopping power, (3) Luminescence decay time and afterglow (persistence), (4) Chemical stability and radiation resistance, (5) Linearity of light response with incident x-ray dose and intensity and(6) Spatial resolution across the screen. Wide band-gap materials are employed for transformation of the x-ray to ultraviolet /visible photons [1].due to the need to detect and monitor also higher energy x- or γ -rays, a bulk scintillator materials were introduced Tl-doped NaI and CsI single crystals [2], which were the first materials developed for this purpose at the end of forties and have been widely used up to the present day due to their high scintillation efficiency.

Kyung CHA[3] studies the effect ofdifferent Tl doping concentrationson the photoluminescence (PL) of (CsI: Tl). The wavelength of the main emission peak was about 550nm, but the light intensity dropped and the emission peak shifted toward the long wavelength for higher Tl concentration in X-ray luminescence case.

Single crystalline columnar CsI (Tl) films demonstrate anincreased scintillation efficiency comparing with thestandard CsI (Tl) single crystalline α-detector at thicknessesmore than 10 mm. [4].

A.S.Tremsin et al[5]did not observe any change in the CsI "crystalline structure or surface morphology after itwas exposed to irradiation with UV-Light, while exposure to very humid airproduces irreversible changes in CsI films.

C.Lu[6]observed thatwhen exposure CsI films to very humid airthe photocathode performance apparently cannot be restored by moderate heating, which helped to restore the QE of the (lms) exposed to relatively dry atmosphere.

The pulse height for thealpha spectra shifted to lower channel numbers with increasing film thickness presumably because of increased light scattering [7].

The UV/Vis Optical data reveals that, CsI film is opaque in the spectral range of 190 nm to 225nm, where as in the spectral range of 225 nm to 900 nm; it is found to be almost transparent[8].

It was found that as themicrocalcification thickness increases the images are more visible. Also, as the thickness of the tissue decreases the structures are less visible because they are very close to each other and the system does not separate them easily as different structures. [9].

The detective quantum efficiency (DQE) which measures the signal-to-noise ratio with comparable thicknesses of CsI and a-Se, the selenium would absorb fewer photons due to its lower atomic number. Also, CsI detectors in a-Si indirect systems have lower additive noise compared to direct systems [10].

Due to the importance of CsI photocathodes, several thin film preparation methods are used in deposition process, such as thermal evaporation technique [11, 12].Ion beam sputteringtechnique [13], e-gun evaporationtechnique [14], spray pyrolysis technique[15], pulsed laser depositiontechnique [16]. Here we report on effect of doping concentration of potassium on characteristic of CsI thin film deposited by chemical spray pyrolysis.

2. Experimental

2.1 Substrate Preparation

CsI were deposited on borosilicate glass slides with dimensions (1.5x1.5cm),which pass through many cleaning stages ,first cleaned in distilled water in order to remove the impurities, second stage rinsing in chromatic acid(for two-day). Third stage the samples were washed repeatedly in deionizer water, finally put in ultrasonic agitation with distilled water for 15min then dried.

2.2 Deposition of the CsI (KI)films

The sample studied here were polycrystalline film CsI layers deposited by spray pyrolysis. CsI powder (1.2gm) from (DEHANE radial deform) 99%puriuty was dissolved in (100ml) ionized water at 30°C using magnetic stirrer for 30min. (0.005gm) of doping material KI powder from (DEHANE radial deform) 99%puriuty was dissolved in (25ml) ionized water at 30°C using magnetic stirrer for 30min.By using micropipette we add respectively (0.25, 0.5, 0.75,1ml) of KI solution to a solutions of(CsI) placed inside a beaker(25ml) with surface area of ($5cm^2$) putting on magnets stirrer for 30min. After that we put the final solution of CsI doped with KI in glass tube of spray system.

We put the deposition substrates over the system substrate at distance of (20Cm) away from the head of nosily spraying, then we rising the substrate temperature to a temperature of deposition. The deposition proses like spraying pulses at time of (4sec) for each pulse with stopping period between each spraying pulse of (26sec) at total spraying time of (60min). Because of the best crystallographic properties of CsI at deposition temperature (200°C) we keep the deposition temperature at (200°C) for all CsI deposition samples as in (fig-1).

2.3 Optical Measurements:

The transmission spectra for all CsI (KI) films were taken in the spectral range of (200 – 900nm) using Phenix-2000 uv-vis spectrophotometer.The absorption coefficient (α) has been calculates by using the following equation [17].

$$\alpha = Ln\frac{1}{T}\frac{1}{d}$$

Where; **d** is the thickness of thin film and **T** is the transmission. The absorption coefficient(**α**) and optical band gap (**Eg**) are related by [18, 19].

$$\alpha h\nu = A(h\nu - Eg)^n \quad \text{..... (2)}$$

Where : **A** is constant depending on transition probability, **h** is Plank's constant, **υ** is the frequency of the incident photon, **Eg** is the band gap of the material and **n** has different values depending on the nature of the absorption process. The plot of $(\alpha h\upsilon)^2$versus hυ gives the best fit results, by extrapolating the liner part down to α = 0, the value of Eg could be determined.The thickness is the single most significant film parameter. It may be measured by in-situ monitoring of the rate of deposition

2.4Thickness measurements

Film thickness is measured by weight method because the thickness of the layer is greater than 1μm.Sensitive electrical balance of Metler AE-160 was used, with preciseness reaches 10^{-4}gm. The following mathematical relationship is adopted

$$Thickness = \Delta m / pf \times A f \quad \text{..... (3)}$$

Δm: represents the deposited thin film weight, which is equal to the difference between weight of the glass slide after and before the deposition process.
pf: density of film.
A f: the film area.

2.5 Structural Measurements

The diffraction spectra of CsI (TI) films were obtained by scanning (2Θ) in the range (20-60) using cu-kα (Philips-PW 1840) which has the following characteristics: the CuKα with (1.540A) wavelength and scanning speed: (3 degree/min).

2-5-1 Crystallite size (***D***) of the polycrystalline material can be calculated from the X-ray spectrum by means of Full Width at Half Maximum (FWHM) method (Scherer relation) [20].

$$D = \frac{0.9\lambda}{\beta cos\theta} \quad \text{..... (4)}$$

Where β is the full – width at half maximum of the XRD peak appearing at the diffraction angle θ.

2.5.2 Dislocation density σ
From the value of grain size we can determine dislocation density [20].

$$\sigma = 1 / D^2 \quad \text{..... (5)}$$

2.5.3 Strain ε
The strain could be calculated by the formula [21].

$$\beta = \left(\frac{\lambda}{D\ cos\theta}\right) - \varepsilon\ tan\theta \quad \text{..... (6)}$$

2.6 Extinction coefficients (K)

The extinction coefficients calculate from the relationship [22].

$$K = \frac{\alpha\lambda}{4\pi} \quad \text{..... (7)}$$

3. Result and Discussion

3.1 Crystallite size and strain by XRD analysis

Typical X-Ray diffract grams of undoped and doped cesium iodide thin films with differentdoping concentration of (K) prepared by spray pyrolysis technique are shown in (Figure 2a, b, c, d, e). No extra diffraction peaks corresponding to CsI phases are detectedIndicating that pure CsI is of polycrystalline, stoichiometric nature. Further, The XRD scan exhibits a number of intense and sharp peaks with lattice plane corresponding to the preferred peaks for CsI crystal are: (110), (200), (211), and (220).The XRD pattern contains an intense peak at Bragg's angle 2ϑ= 27.06, assigned to (110) crystallographicplane and three other XRD peaks are alsofound at Bragg's angles 2ϑ= 38.87, 48.30 and 56.49corresponds to (200), (211) and (220) crystallographicplanes, respectively. These crystallographic planes attributed a body centered cubic (bcc) structure.

The intensity of peaks decrease with increasing doping concentration,according to increasing the grain size and the defects that produce due to the packing mismatch because of impurities during deposition. All of this could be attribute to the residual stresses that generate defects which casing deformations like dislocations in the film as in fig(3).We observe the peak of (110) lattice plane ismost intense peaks, and has a good stability without any shift in angle(2θ=

27.06). The value of full width at half maximum (FWHM) and 2θ is corresponding to peaks for variousand the inter-planer spacing (d) with comparing it with standard d-value taken from ASTM diffraction data file. To the most intense (110) peak for various doping concentration of (K)of thin CsI films are shown in Table 1.

Fig (4) illustrated that at increasing doping concentration of (K) from (0.25-0.75ml) lead to a very little increase in the preparation crystal size, while a large increase in grain size occur at concentration (0.75-1ml) the increase in grain size at fixed doping weight be attributed to the preferentially substitutional incorporation of dopant atoms, sample with doping concentration(1ml) has a higher grain size than the rest samples, which lead to decrease the dislocation density as in fig(5), and causing decrease number of layers casing to reduce the strain in the film Fig (6).

From Fig (7) which represent the relationship of CsI (KI) films transmittance at wavelength range (200 – 800nm), we can see a decrease in transmittance value with increasing value of doping concentrationat wavelength range (200 – 400nm) due to the process of doping which increase the absorbance of the film, this may be due to the highest ionization energy of impurities(deep impurities) , then the transmittance will saturate at wavelength above (360nm) which means that CsI(K) film have a large transmittance value at wavelength (360nm)having more than 80%transmittancya sharp increase in transmittance near a wavelength (360 nm) is indicating its crystalline nature.

Fig (8) represents the extinction coefficient for CsI (K) films at different doping concentration of (K). The extinction coefficient represent the quantity of energy that absorbed in the film, which means the quantity of extinction for electromagnetic wave inside the material and depend on free electrons density and structure defects. The extinction coefficient for CsI (K) films deposited withdoping concentration of (K)(1ml)is much less than that deposited with (0.75, 0.5, and 0.25) at wavelength200< λ <400nm, and sharp decrease in 240nm at IR region, this may be due to decrease the energy gap for films.Fig (9) shows the absorption coefficient, where the sharp decrease in (α) with increasing (λ).

From the observed absorption data, it is found that the plot of $(\alpha\ h\upsilon)^2$ versus (hυ) fig (10) give fairly near straight line indicating that the transition were direct and allowed. Band gap (Eg) is obtained by extrapolation to zero absorption.Increasing the doping concentration of (K) lead to decrease energy gap may be due to creating defects or vacancies which lead to change in energy gap [22].

In fig (11) shows the angular dependence of the average grain size of doped sample with undoped as reference material. It is clear that the grain size of the different reflection planes is larger for undoped. The grain size is more pronounced in 110 reflection plane where grain size attained a value of at 1*ml* K, the increase in grain size at fixed doping concentration is due to the preferentially substitutional incorporation of dopant atoms [23].

The plot of the inter-planer spacing (d) as a function of 2θ presented in fig (12), it is immediately apparent that the d-spacing is strongly dependent on the reflection plane. Doping lead to slight changes in the calculated by doping. This is usually attributed to compressive stress in plain parallel to the surface [24].

The variation of FWHM versus 2θ (instrumental resolution functions) obtained for sample with different doping concentration is shown in Fig(13) together with that belonging to undoped it indicates the strong structural line broadening of the undoped, while the angular dependence of the doped sample was found to vary in the same manner far from linear. The plot displays great broadening which implies that in these samples size and strain effects are significant.

4. Conclusion

In summary we studied the effect of K ions deponent on the structure properties of CsI films. The results show a decrease in values of peak intensity with rising doping ratio of K ions, with increasing Grain size, and decreasing dislocation and strain of films. The value of energy gap decrease with increasing dopant ratio.

Table 1: Structural parameters of CsI (K) film analyses from XRD:

Orientation	2θ(deg)	D(°A)Present study	D(°A)Astm value	FWHM
110	27.5	3.228	3.23	0.5942
200	38.3	2.282	2.284	0.4431
211	48.8	1.863	1.865	0.4430
220	57	1.613	1.615	0.4461

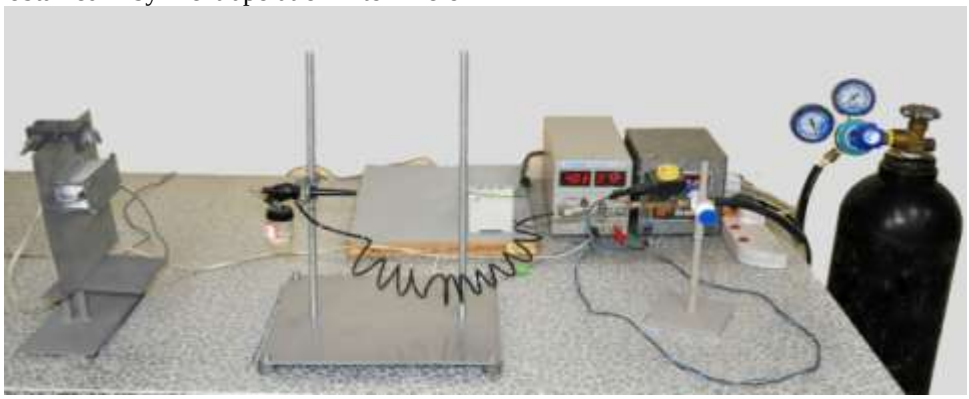

Figure 1: Photograph of spray pyrolysis deposition technique

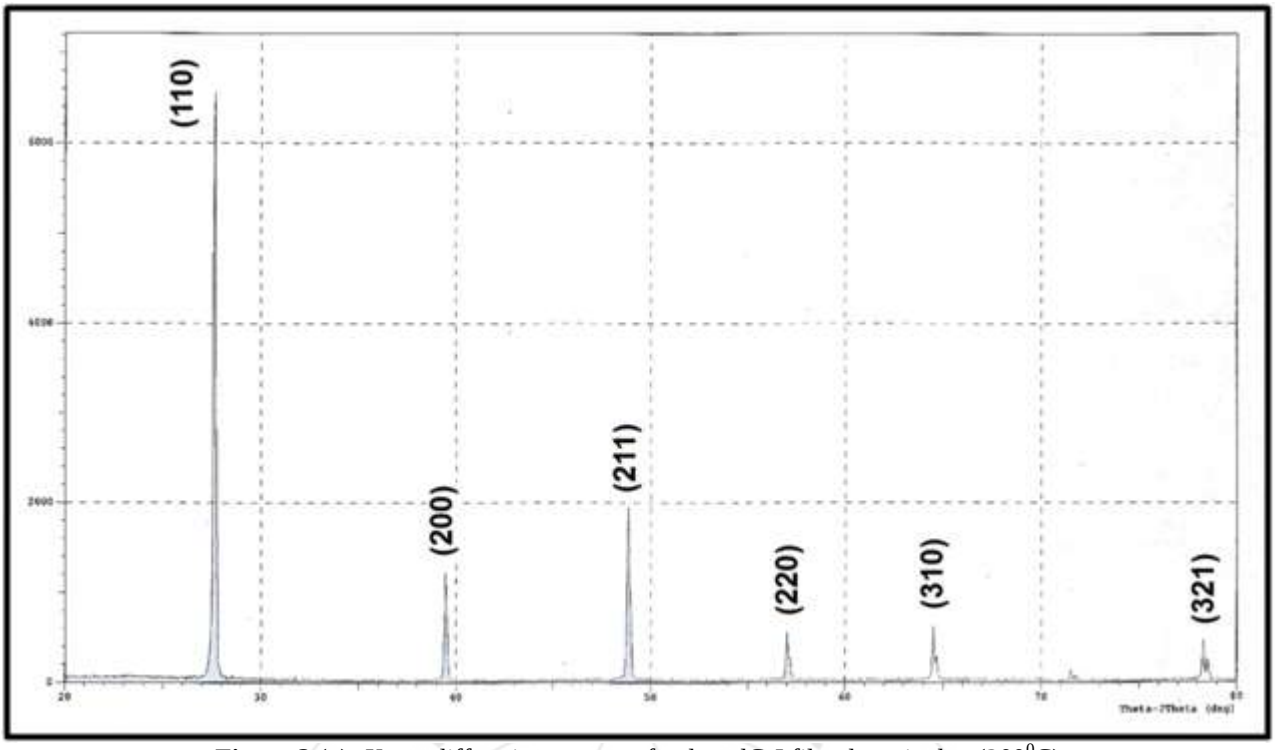

Figure 2 (a): X-ray diffraction pattern ofundopedCsI film deposited at (200^{0}C)

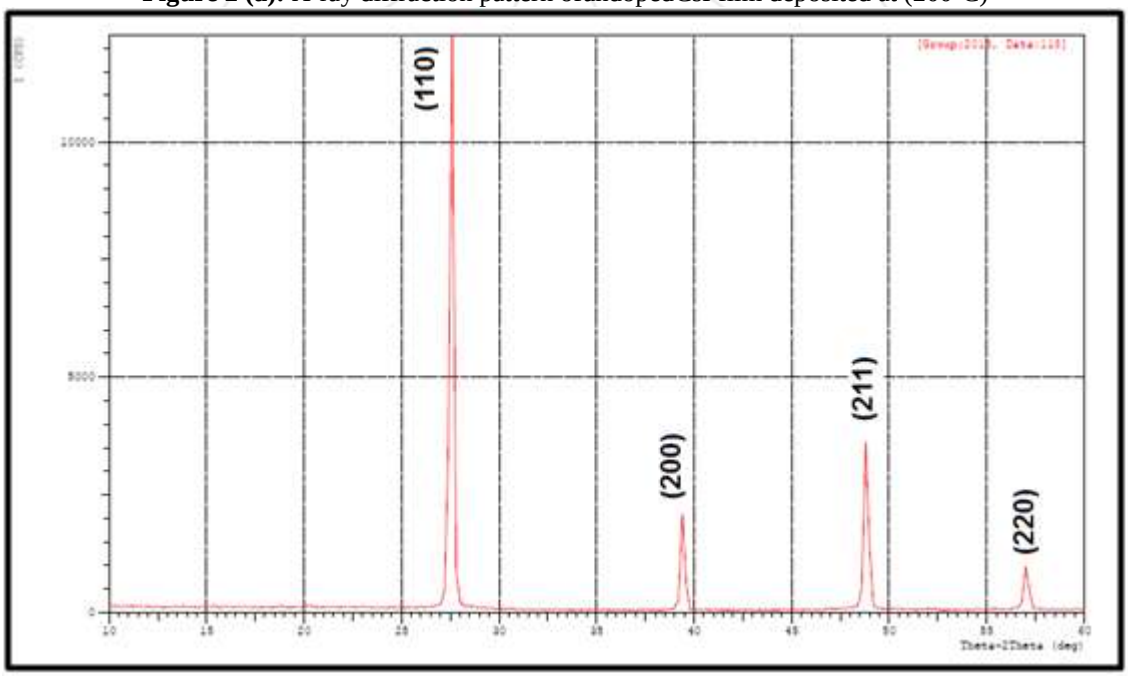

Figure 2 (b): X-ray diffractionpattern of CsI film deposited at (200^{0}C) doped with (0.25)ml KI

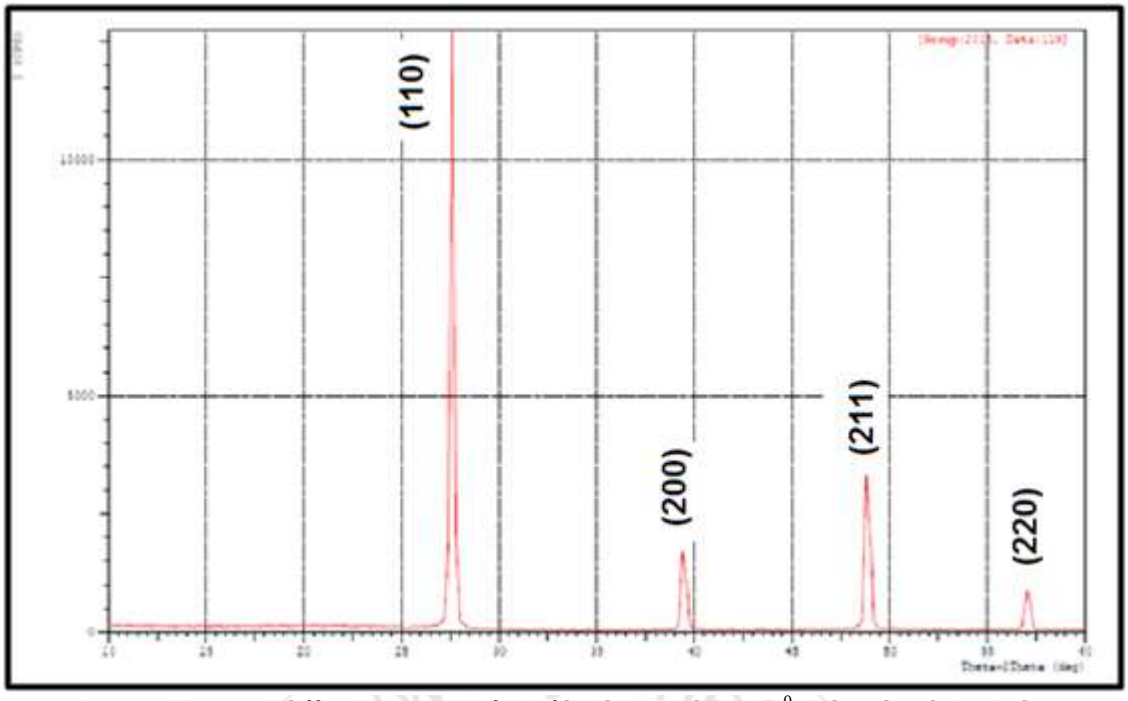

Figure 2 (c): X-ray diffractionpattern of CsI film deposited at (200^{0}C) doped with (0.5)ml KI

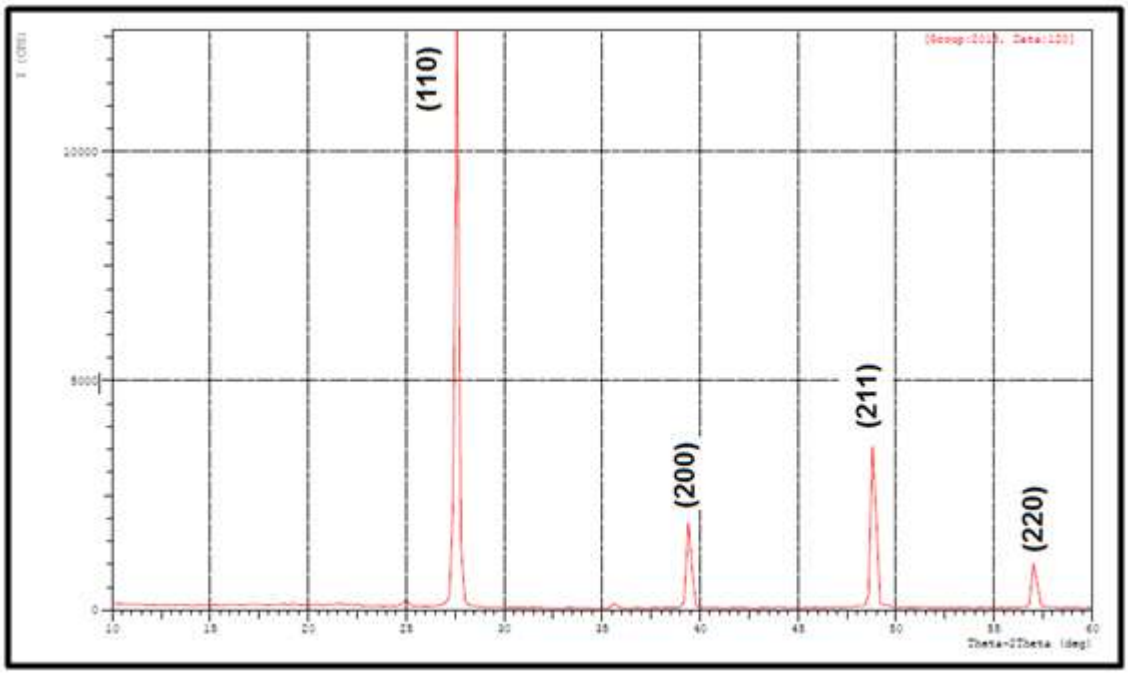

Figure 2 (d): X-ray diffractionpattern of CsI film deposited at (200^{0}C) doped with (0.75)ml KI

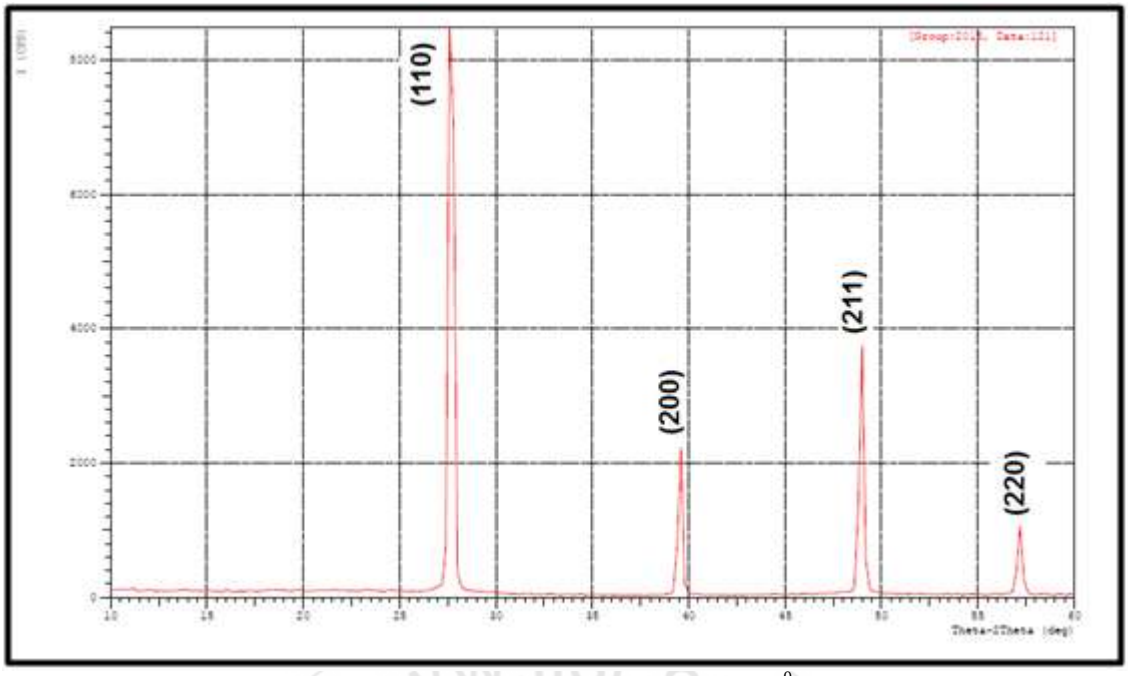

Figure 2 (e): X-ray diffractionpattern of CsI film deposited at (200^{0}C) doped with (1.0)ml KI

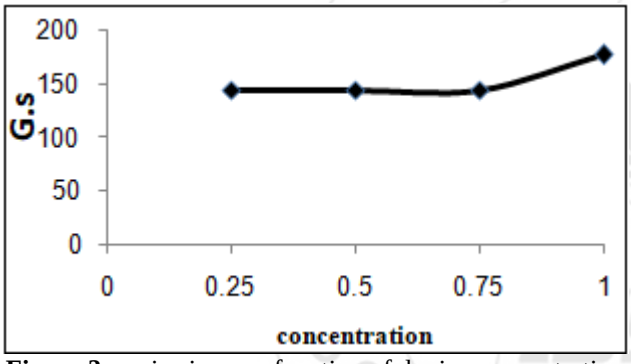

Figure 3: grain size as a function of doping concentration

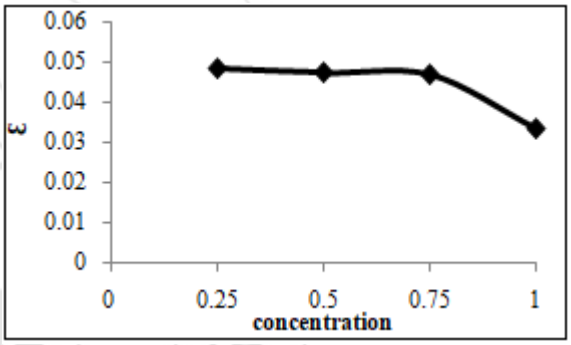

Figure 5: Effect ofdoping concentration on strain established on CsI films

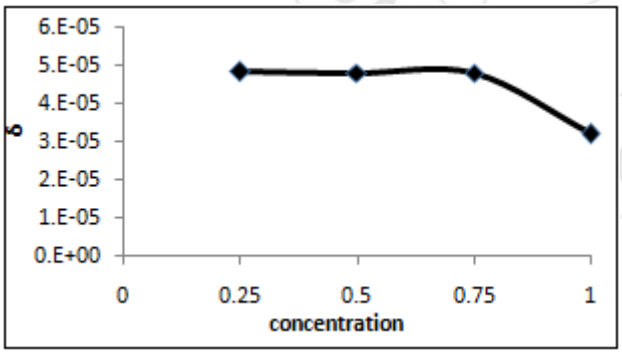

Figure 4: Dislocation density curves as a function of doping concentration

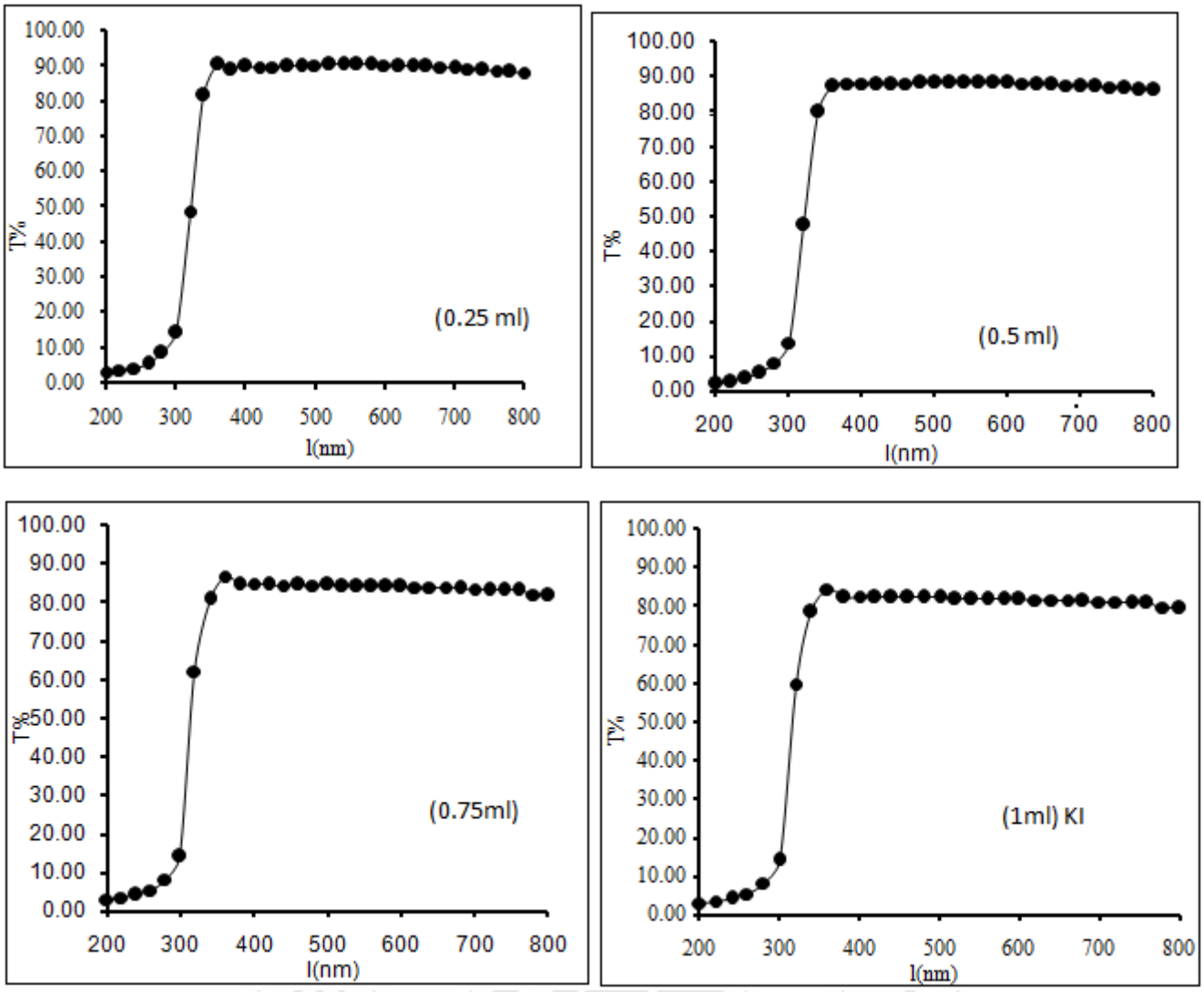

Figure 7: Transmission plots of CsI films with different doping concentrations

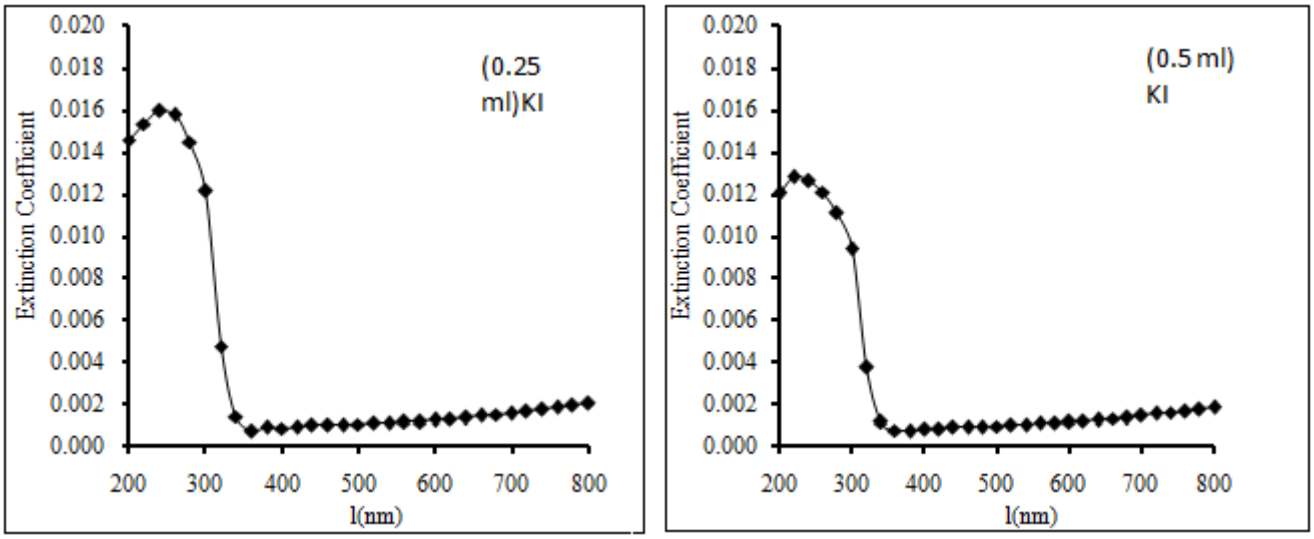

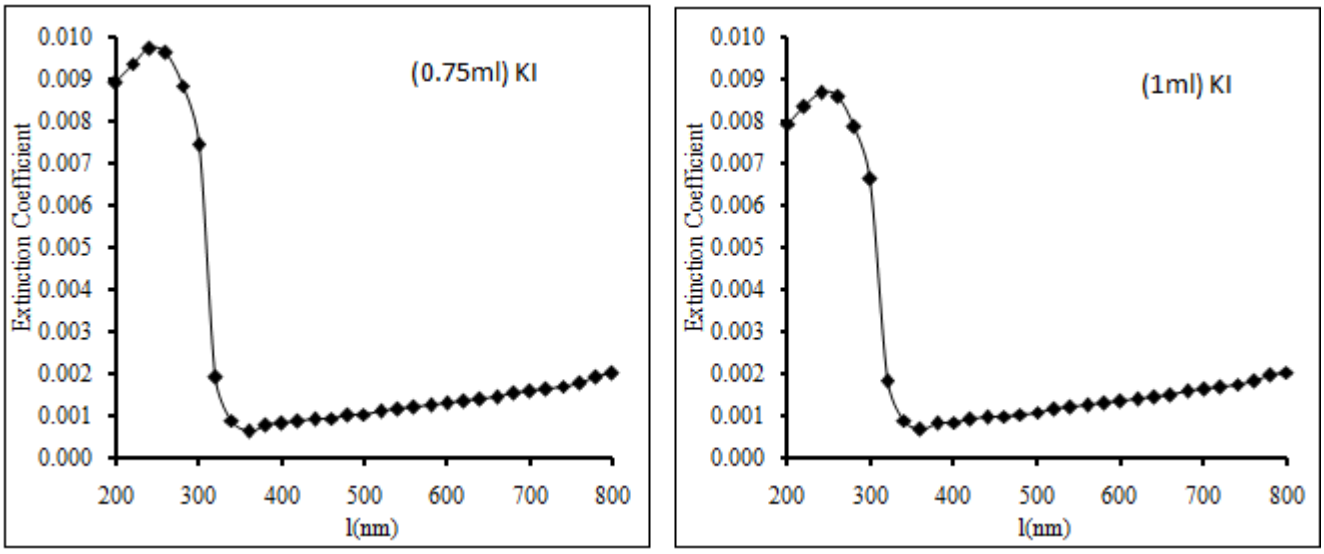

Figure 8: Extinction coefficient plots of CsI films with different doping concentrations

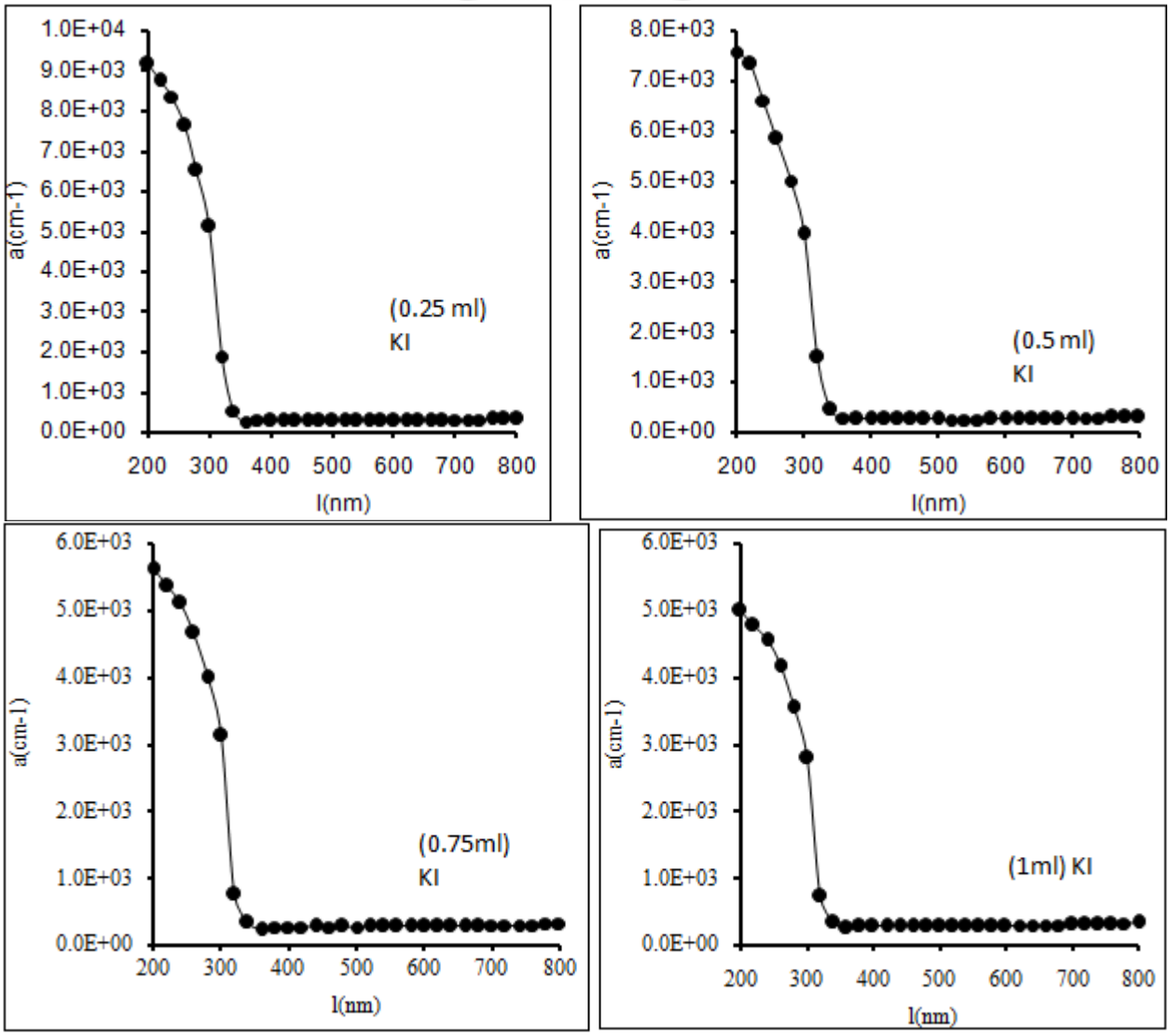

Figure 9: Absorption Coefficient plots of CsI films with different doping concentrations

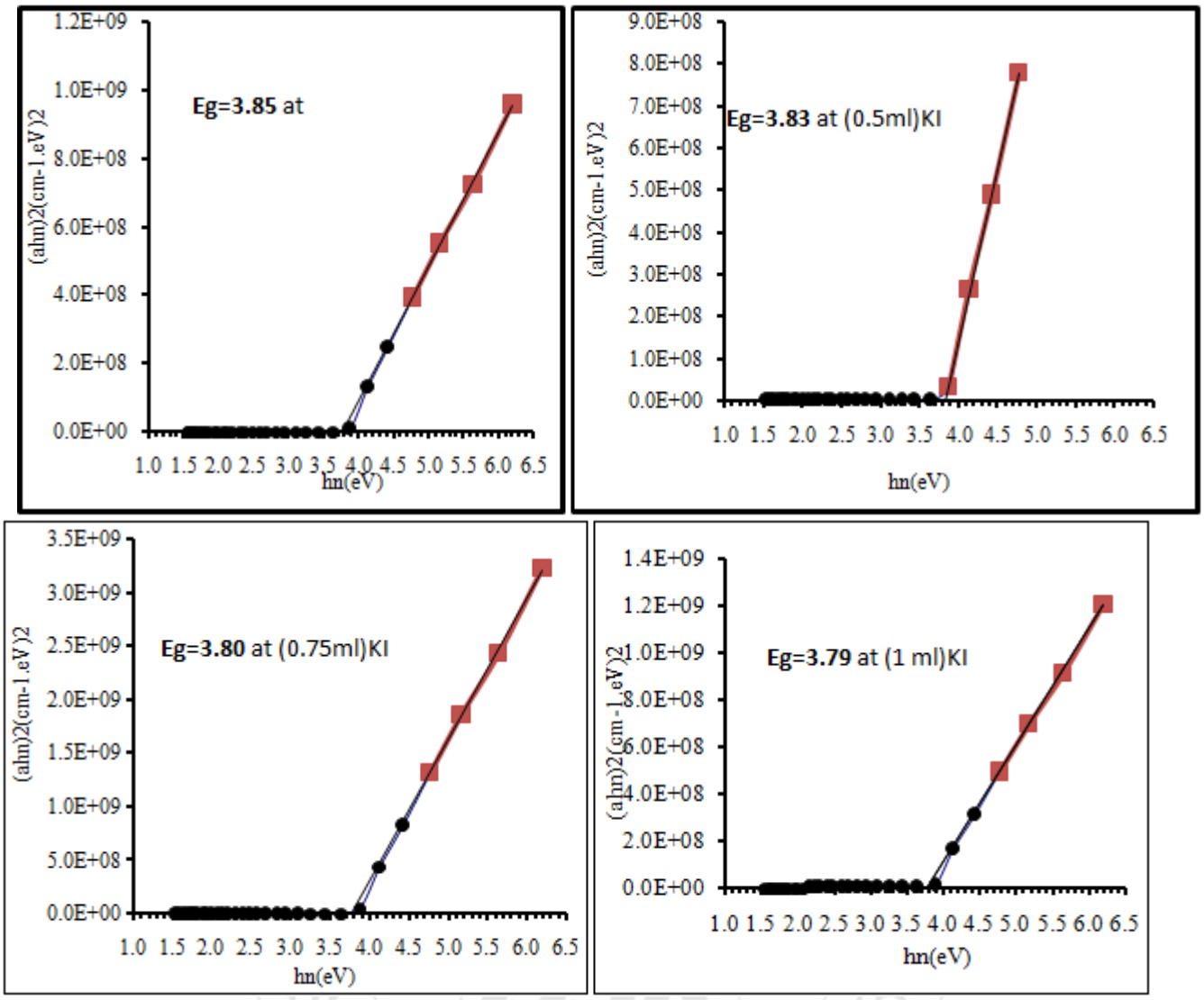

Figure 10: Variation of Energy gap plots of CsI films with different doping concentrations

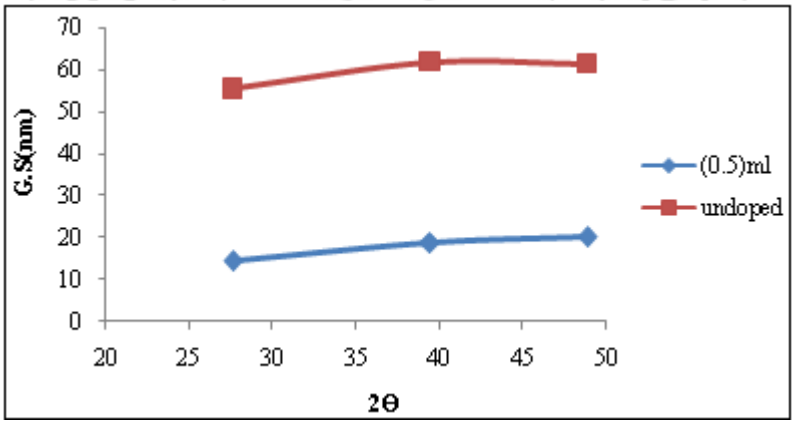

Figure 11: Grain size curves for CsI angular dependence of undoped and doped samples

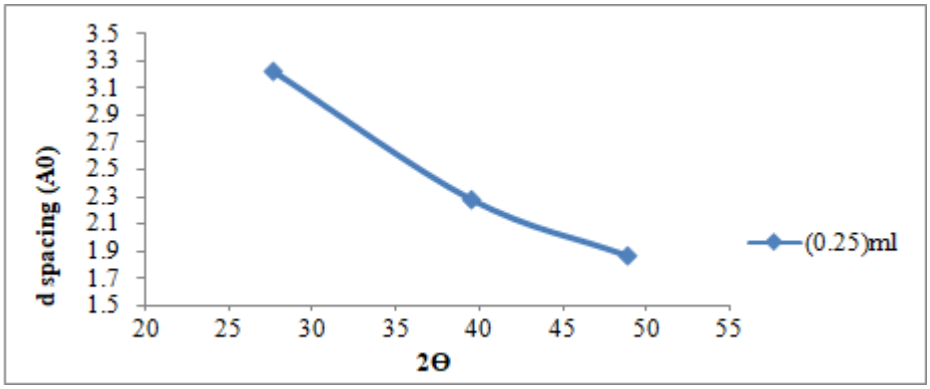

Figure 12: d-Spacing curves for CsI films with 2ɵ

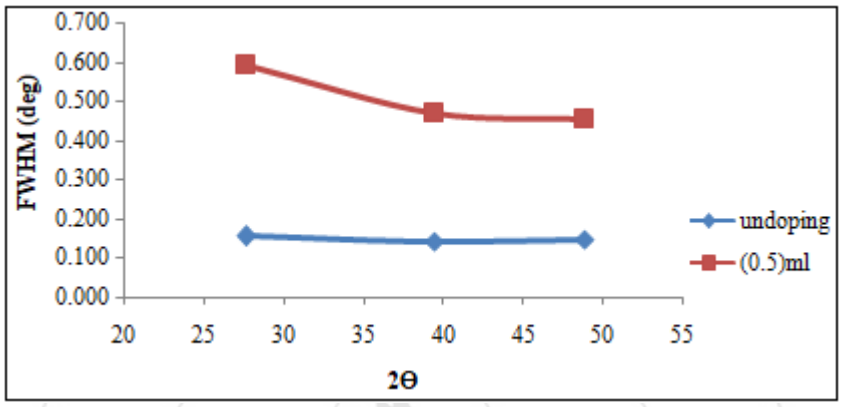

Figure 13: FWHM parameter as a function of 2θof undoped and doped samples

References

[1] Martin Nikl, Meas. Sci. Technol. **17** (**2006**) R37–R54
[2] Editors notes (**1950**) Properties of scintillation materials*Nucleonic* 70–3VanSciverW and Hofstadter R (**1951**) Scintillations in thallium-activated CaI_2 and CsI *Phys. Rev.* **84** 1062–3
[3] KYUNG CHA, Bo,8th International Conference on Position Sensitive Detectors. September (**2008**).
[4] A. Ananenko, A. Fedorov, A. Lebedinsky, P. Mateychenko, V. Tarasov, Yu. VidajSemiconductor Physics, Quantum Electronics & Optoelectronics. (**2004**). V. 7, N 3. P. 297-300.
[5] A.S. Tremsin, S. Ruvimov, 1, O.H.W. Siegmund! Nuclear Instruments and Methods in Physics Research A 447 (**2000**) 614}618.
[6] C. Lu, K.T. McDonald, Nucl. Instr. and Meth. A 343(**1994**) 135.
[7] Seema Shinde. Proceedings of the DAE Symp. On Nucl. Phys. 59 (**2014**).
[8] Triloki, R. Rai, Nikita Gupta, Nabeel F. A. Jammal, B. K. Singh, arXiv: 1409.5290v2 [physics.ins-det] 16 Jan **(2015).**
[9] Vasiliki A. Spyropoulou1, Nektarios Kalyvas1, 2, Anastasios Gaitanis1, 2, Ioannis S.Kandarakis2*, George S. Panayiotakis1,e-journal of science &Technology (2) ,(5), pp. (58-62),April(**2010**).
[10] Bassir, C., Fischbach, F., Felix, R., Freund, T., Pech, M., Ricke, J., & Werk, M. **(2003).** Comparison of Indirect CsI/a:Si and Direct a: Se Digital Radiography An assessment of contrast and detail visualization. *Acta Radiologica*, *44*(6), 616-621. doi:10.1046/j.1600-0455.2003.00137.x
[11] V M Brendel, S V Garnov, T F Yagafarov, L D Iskhakova and R P Ermakov.Quantum Electronics, Volume 44, Number 9, (**2014**).
[12] V. Dangendorf et al., Nuclear Instruments and Methods A 289 (**1990**) 322-324.
[13] M.A. Nitti et al., Appl. Phys. A 80, (**2005**) 1789-1791.
[14] P. Maier-Komor et al., Nuclear Instruments and Methods A 362 (**1995**) 183-188.
[15] S.O. Klimonsky et al., Inorganic materials, (**2011**) 47 pp1033-1038.
[16] S.B. Fairchild et al., J. Vac. Sci. Technol. A 29 (**2011**) 031402.
[17] S. M. Sze," Physics of Semiconductor Devices", Second Edition, John Wiley and Sons, New-York, (**1981**).
[18] H. Reiss, P. Mirabel, R. L. Whetten; J. Phys. Chem. 92(**1988**)7241.
[19] N. F. Mott, E. A. Daves," Electronic Processes in Noncrystalline Materials; Oxford, Clarendon Press (**1979**)27.
[20] B.D.Cullity and SR. S tock, Elements of X-Ray Diffraction, Third edition Prentice-Hall in the United States of America, (**2001**).
[21] G.B.williamson, R.C.Smallman, philos.Mag.1 (**1956**)34
[22] K.Chopra, and L.Malhorta, thin film technology and applications, 13 (**1984**) 117-120.
[23] J.Kucytowski, wokulska: Dryst.Res.Technol. 40 (**2005**) 424.
[24] A.Asadov, W.Gao, Z.Li, M.Hodgson, Thin solid films 476 (**2005**) 201.